Eng. & Technology, Vol.25, No.4, 2007

Experimental and Numerical Studies on Water Cooling Tower Performance

Asst. Prof.Dr. Waheed Sh.Mohammad* Prof.Dr. Jalal M. Jalil*
Asst.Lecturer.Essam O. Ali

Received on: 5/4/2005
Accepted on; 22/1/2007

Abstract

Theoretical and experimental studies were conducted on forced draft water cooling tower. In such towers, the heat and mass transfer take place from the hot water to the bulk air, which passes through the tower. The theoretical study includes two parts, the first part describes the numerical solution for the water cooling tower governing equations, a two dimension air momentum equation (Navier-Stocks equations) and air enthalpy equation (energy equation), moisture content and water enthalpy equation. The effect of turbulence was simulated using the k-ε model. The packing-air resistance is described and added to the air momentum equation in y-direction only. The second part highlights the use of three different packing types. This includes the use of a ceramic packing in two different heights (0.66, 0.48m) in addition to an aluminum packing. A simple comparison between all the above types of packing behavior is conducted. The experimental study was conducted using Hilton water cooling tower, which is a counter flow type. The variation in many variables, which affect the tower efficiency, are described in this part of the research including variation heating loads, entering water mass flow rates and incoming air volume flow rates. The flow field velocity vector for air through the tower is plotted, and an accurate behavior of both air and water properties was found.

الخلاصة

تم إجراء دراسة نظرية وعملية لأبراج تبريد الماء القسرية. حيث يحدث انتقال الحرارة والكتلة من الماء الساخن إلى الهواء المار خلال البرج. الدراسة النظرية شملت جانبين, الجانب الأول تضمن معالجة عددية للمعادلات الحاكمة والخاصة بعمل هذه الأبراج. مثال على ذلك حل معادلات حفظ الكتلة للماء والهواء على حد سواء وكذلك معادلات حفظ الزخم وهي معادلات (Navier-Stockes) ذات البعدين ومعادلات حفظ الطاقة وتمثلت بمعادلتي المحتوى الحراري والمحتوى الرطوبي للهواء ومعادلة المحتوى الحراري للماء , حيث تم حل المعادلات الذكورة أعلاه باستخدام طريقة الفروق المحددة (Finite Difference). تم تمثيل الاضطراب من خلال استخدام (K-ε) مود يل. كذلك كان لتأثير مقاومة الحشوة لسرعة جريان الهواء خلال البرج نصيبا من هذه الدراسة حيث تم حسابه وإضافة الحد الخاص به إلى معادلة الزخم باتجاه أل (y) فقط. أما الجانب الثاني فقد جاء موضحا الاستخدام النظري لثلاثة أنواع من الحشوات, حيث تضمن استخدام حشوة سيراميكية بارتفاعين مختلفين (0.66 and 0.48 m) بالإضافة إلى الحشوة الأصلية من الألمنيوم. حيث أجريت مقارنة مبسطة بين نتائج الأنواع الثلاثة الذكورة آنفا, وتم الحصول على نتائج مقبولة من خلال إجراء هذه المقارنة. الدراسة العملية أجريت من خلال استخدام برج التبريد نوع (Hilton) والذي هو من النوع القسري ذو الجريان المتعاكس. تضمنت هذه الدراسة دراسة تأثير متغيرات عديدة وكل ما من شانه أن

http s://doi.org/10.30684/etj.25.4.1
2412-0758/University of Technology-Iraq, Baghdad, Iraq

يحسن كفاءة برج التبريد, مثال على ذلك معدل تدفق الماء الساخن إلى البرج, معـــدل التـــدفق الحجمي للهواء المار خلال البرج إضافتا إلى دراسة الحمل الحراري. تم إيجاد تخمـــين دقيـــق لحقل الجريان (Flow-Field) للهواء خلال البرج وكذلك إيجاد تخمين دقيق لتصرف خـــواص الهواء والماء ومعدل الحرارة والكتلة المنتقلة من الماء إلى الهواء. كذلك تم التوصل إلى كل ما من شانه أن يحسن كفاءة أبراج التبريد وهو طبيعة شكل ومعدن الحشوة المستخدمة إضـــافتا إلى معدل التدفق الحجمي للهواء الداخل إلى البرج.

NOMENCLATURE

$q^{\bullet m}$	Rate of heat transfer per unit volume	w/m^3
$m_v^{\bullet m}$	Rate of mass transfer per unite volume	$kg/m^3.s$
k	Mass transfer coefficient	$kg/m^2.s$
a	Area of transfer surface per unit volume	m^2/m^3
h_{sw}	Specific enthalpy of saturated moist air	kJ/kg
h_a	Specific enthalpy of moist air	kJ/kg
w_{sw}	Moisture fraction of saturated moist air	kg_v/kg_{da}
u	Horizontal air velocity component	m/s
v	Vertical air velocity component	m/s
u_f	Water velocity	m/s
P	Pressure	Kpa
g	Gravitational acceleration	m/s^2
f_y	Resistance to air flow in y-direction	N/m^3
h_f	Specific enthalpy of water	kJ/kg
W_G	Air molecular weight	
R	Universal gas constant	$J/(kg-mol.K)$
x	Horizontal Cartesian coordinate	m
y	Vertical Cartesian coordinate	m
K	Turbulent Kinetic energy	m^2/s^2
v_t	Turbulent Kinematics viscosity	m^2/s
i, j	Grid point places in directions (x,y) respectively	

a_e, a_w, a_s, a_n	Differential equation coefficients in x-direction	kg/s
b_e, b_w, b_s, b_n	Differential equation coefficients in y-direction	kg/s
d_e, d_w, d_s, d_n	Differential equation coefficients	kg/s
e_e, e_w, e_s, e_n	Differential equation coefficients	kg/s
u^*, v^*	Stared velocity components	m/s
$u^/, v^/$	Correction velocity components	m/s
P^*	Stared pressure	Kpa
$P^/$	Correction pressure	Kpa
l_n, l_s	Differential equation coefficients	kg/s
C_w	Water specific heat	$kJ/kg.K$
$m_w^\bullet$	Mass flow rate of water per unit plan area of packing	$kg/m^2.s$
$m_a^\bullet$	Mass flow rate of air per unit plan area of packing	$kg/m^2.s$
t_f	Water temperature	C^o
V	Volume occupied by packing per unit plan area of packing	m^3/m^2

GREEK LETTERS

r	Moist air density	kg/m^3
r_f	Water density	kg/m^3
m_{eff}	Effective viscosity	$kg/m.s$
r_{amb}	Ambient air density	kg/m^3
Γ_{eff}	Effective exchange coefficient	$kg/m.s$
f	The dependent variable	
Γ_Φ	Diffusion term	$N.s/m^2$
S_f	Source term	
s_{eff}	Effective Prandtl number	
e	Disspasion rate coefficient	m^3/s

C_m, C_{1e}, C_{2e}	Turbulent empirical constants	
m_t	Turbulent dynamic viscosity	$N.s/m^2$
Γ_k	Defusion term for Kinetic energy equation	$N.s/m^2$
Γ_e	Defusion term for dissipation rate equation	$N.s/m^2$
s_k	Prandtl number for Kinetic energy equation	
$\mathbf{l}$	Length scale	m
s_e	Prandtl number for dissipation rate equation	

1. INTRODUCTION

Majumdar, A. et al, (1983)[1]. discuss the limitations of current practices of evaluating thermal performance of wet cooling towers and describes a more advanced mathematical model for mechanical and natural draft cooling towers. Burger, (1989)[2], studied a various elements of the modern cross – flow cooling tower and their upgrading capability. Alwan, (1991)[3], studied the counter–flow water cooling tower with flat plate asbestos packing. Al. Habobi, (1995)[4], studied the performance of ceramic blocks and asbestos sheets used as a packing for a counter – flow water cooling tower. Mohiuddin and Kant, (1996)[5], described the detailed methodology for the thermal design of wet, counter – flow and cross – flow types of mechanical and natural draft cooling towers. Al–Nimr, (1998)[6], studied a dynamic thermal behavior of a counter–flow cooling tower by proposed a simple mathematical model. Bedekar, et. al, (1998)[7], studied experimentally the performance of a counter–flow packed–bed mechanical cooling tower. Gan and Riffat, (1999)[8], presented a numerical technique for evaluating the performance of a closed wet cooling tower for chilled ceiling systems. Al. Nimr, (1999)[9], studied the dynamic thermal behavior of counter–flow cooling towers that contain packing materials. Abdula, (2002)[10], conducted a numerical study for forced draft cooling towers.

A forced draft counter flow water cooling towers will be employed. A theoretical and experimental study will be carried out on this tower. In theoretical part a thermal solution (heat and mass balance) will be used to solve many equations using finite difference method based on computational fluid dynamics (CFD) such equations are, X – direction momentum equation, Y –direction momentum equation, air enthalpy equation, air moisture fraction equation, water enthalpy equation, K–Є model for turbulent flow and equation of state. The effect of packing type heightens air flow rate, water flow rate and heating load on the tower performance will be predicted. Experimentally several tests on a counter–flow cooling tower test plant will be conducted. These tests will quantify the previous effects and justify the CFD program.

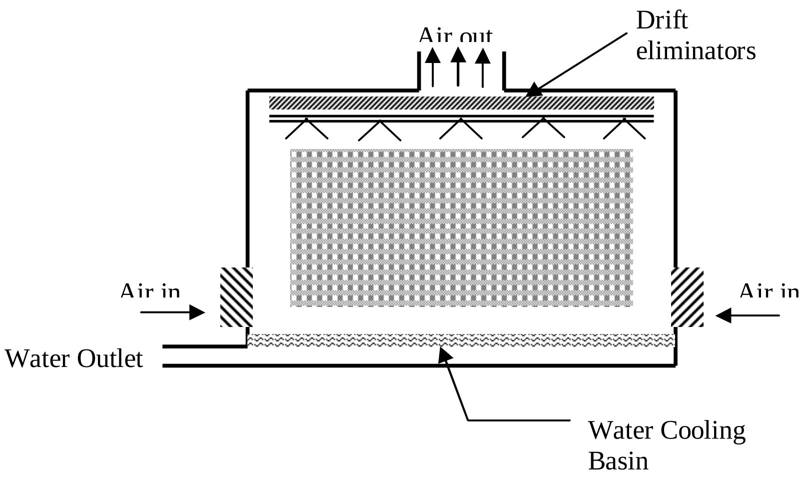

Fig. (1) Configuration of the counter flow water cooling tower.

2. GOVERNING EQUATIONS

The basic equations that describe the flow of the fluid, heat and mass transfer between water and bulk air in two dimention with Cartesian coordinate system are the continuity, the Navier-Stokes and energy equations[1].

(1) Continuity equation (Mass of Air).

$$\frac{\partial}{\partial x}(ru)+\frac{\partial}{\partial y}(rv)=m_v^{\bullet m} \quad \text{.........................(1)}$$

(2) Continuity equation (Mass of Water).

$$\frac{\partial}{\partial y}(r_F u_F)=m_v^{\bullet m} \quad \text{...............................(2)}$$

(3) X-Direction momentum equation.

$$\frac{\partial}{\partial x}(ruu)+\frac{\partial}{\partial y}(rvu)=2\frac{\partial}{\partial x}\left(m_{eff}\frac{\partial u}{\partial x}\right)+\frac{\partial}{\partial y}\left(m_{eff}\frac{\partial u}{\partial y}\right)+\frac{\partial}{\partial y}\left[m_{eff}\frac{\partial v}{\partial x}\right]-\frac{\partial P}{\partial x} \quad \text{.........(3)}$$

(4) Y-Direction momentum equation.

$$\frac{\partial}{\partial x}(ruv)+\frac{\partial}{\partial y}(rv^2)=-\frac{\partial P}{\partial y}+2\left[\frac{\partial}{\partial y}\left(m_{eff}\frac{\partial v}{\partial y}\right)\right]+\frac{\partial}{\partial x}\left[m_{eff}\frac{\partial v}{\partial x}\right]+\frac{\partial}{\partial x}\left[m_{eff}\frac{\partial u}{\partial y}\right]-g(r-r_{amb})-f_y \quad \text{..................................(4)}$$

(5) Air enthalpy.

$$\frac{\partial}{\partial x}(ruh_a)+\frac{\partial}{\partial y}(rvh_a)=\frac{\partial}{\partial x}(\Gamma_{eff}\frac{\partial h_a}{\partial x})+\frac{\partial}{\partial y}(\Gamma_{eff}\frac{\partial h_a}{\partial y})+\dot{q}''' \quad \text{....(5)}$$

(6) Moisture Fraction equation.

$$\frac{\partial}{\partial x}(ruw_a)+\frac{\partial}{\partial y}(rvw_a)=\frac{\partial}{\partial x}(\Gamma_{eff}\frac{\partial w_a}{\partial x})+\frac{\partial}{\partial y}(\Gamma_{eff}\frac{\partial w_a}{\partial y})+\dot{m}_v''' \quad \text{.............(6)}$$

(7) Water enthalpy equation.

$$\frac{\partial}{\partial y}(r_F u_F h_w)=-q^{\bullet m} \quad \text{...............(7)}$$

Because the density varies along the tower, equation of state should be used.

$$r=\frac{P.w_G}{R.(t_{adb}+273)} \quad \text{................(8)}$$

TURBULENCE MODEL (k-e)

The k-e model characterizes the local state of turbulence by two parameters, the turbulent Kinetic energy, k and the rate of its dissipation, e . The Kinematics viscosity is related to these parameters by Kolmogrov-Prandtl expression:

$$v_t = C_m \frac{k^2}{e} \text{.......................(9)}$$

where C_μ is an empirical constant. The distribution of k and e over the flow field is calculated from the following semi-empirical transport equations for k and e [12].

A- Turbulent Kinetic energy:

$$\frac{\partial}{\partial x}(ruk)+\frac{\partial}{\partial y}(rvk)=\frac{\partial}{\partial x}\left(\Gamma_k\frac{\partial k}{\partial x}\right)+\frac{\partial}{\partial y}\left(\Gamma_k\frac{\partial k}{\partial y}\right)+m_t\left[2\left(\frac{\partial u}{\partial x}\right)^2+2\left(\frac{\partial v}{\partial y}\right)^2+\left(\frac{\partial u}{\partial y}+\frac{\partial v}{\partial x}\right)^2\right]-e\text{..(10)}$$

where

$$\Gamma_k = \frac{m_{eff}}{s_k}, e = \frac{C_m.k^{3/2}}{l} \text{...........(11)}$$

B- Rate of dissipation rate equation:

$$\frac{\partial}{\partial x}(rue)+\frac{\partial}{\partial y}(rve)=\frac{\partial}{\partial x}\left(\Gamma_e\frac{\partial e}{\partial x}\right)+\frac{\partial}{\partial y}\left(\Gamma_e\frac{\partial e}{\partial y}\right)+C_{1e}\frac{e}{k}m_t\left[2\left(\frac{\partial u}{\partial x}\right)^2+2\left(\frac{\partial v}{\partial y}\right)^2+\left(\frac{\partial u}{\partial y}+\frac{\partial v}{\partial x}\right)^2\right]-C_{2e}\,r\frac{e^2}{k}\text{...........................(12)}$$

where

$$\Gamma_e = \frac{m_{eff}}{s_e} \text{..........................(13)}$$

The empirical constants appearing in the above model are shown in the following table.

Table (1) Empirical constants in the k-e

C_m	C_{1e}	C_{2e}	s_k	s_e
0.09	**1.44**	**1.92**	**1.00**	**1.30**

Cooling tower – governing equations are non-linear and required to be iterative procedure, However these equations must be written in a general form that is:

$$\frac{\partial}{\partial x}(ru\Phi)+\frac{\partial}{\partial y}(rv\Phi)=\frac{\partial}{\partial x}\left(\Gamma_\Phi\frac{\partial \Phi}{\partial x}\right)+\frac{\partial}{\partial y}\left(\Gamma_\Phi\frac{\partial \Phi}{\partial y}\right)+S_\Phi\text{......................(14)}$$

where Φ is the dependent variable, which may be a directional quantity such as velocity components (u,v) or scalar quantity such as temperature or enthalpy (h_a). The left side of equation (14) is the convection term which mean the fluid transfer, the right side is the diffusion term which gives the variation in fluid property during the flow, S_Φ is the source term which means the source of heat, mass transfer or pressure variation that allows fluid to flow, Γ_Φ is the diffusion coefficient which is a dynamic viscosity in momentum equation but effective exchange coefficient in enthalpy and moisture fraction equations[11], and

$$\Gamma_{eff} = \frac{m_{eff}}{s_{eff}} \text{....................................(15)}$$

where s_{eff} is the Prandtl number, which takea unit. Equation (14) is solved by using a finite volume method, which divided the flow field in to small volumes, and integration of this equation on the faces of the control volume is the key solution of this method.

4. NUMERICAL SOLUTION

The resulting equation after discretization is:

$$a_j\Phi_j = a_w\Phi_W + a_e\Phi_E + a_n\Phi_N + a_s\Phi_S + S_{\Phi j}\ldots\ldots\ldots\ldots\ldots\ldots\ldots\ldots(16)$$

and for water enthalpy, equation (17) is a numerical solution result.

$$l_j h_{wj} = l_n h_{wn} + l_s h_{ws} + S_{hwj}\ldots\ldots..(17)$$

where a_j, a_w, a_e, a_n, a_s is coefficient $\Phi_j, \Phi_W, \Phi_E, \Phi_N, \Phi_S$. The pressure is corrected to satisfy continuity at the end of each iteration. To derive the pressure correction equation we define the following[11]:

$$P = P^* + P^/ : u = u^* + u^/ : v = v^* + v^/$$

$$\Phi_j = \Phi_j^* + \frac{P_w^/ - P_e^/}{A_j}\ldots\ldots\ldots\ldots(18)$$

where, the starred values (u^*, v^*) represent the flow solution given by the pressure (P^*). By applying the above in the discretized momentum and continuity equations and simplifying, a linear system can be obtained for $P^/$ (Pressure correction) in solving the steady momentum equations in this step, under-relaxation factor of (0.5) is applied to the velocity components to prevent instability and divergence due to non-linearity in the Navier-Stokes equation. Also under-relaxation factor of (0.8) is used for pressure correction. After steady state solution is obtained for the flow field[12].

4. EXPERIMENTAL WORK

The experimental work was carried out using Hilton water-cooling tower, which is a forced draft counter flow type. The tower was equipped with four heaters (2.5 kw each) to heat the water and that represents the load on it. The tower was equipped also with several measuring devices to express the condition of water and air at inlet, outlet and other five stations along the tower[13].

The equations reflect mass and heat balance at any point in the tower is:

$$\frac{ka.V}{\overset{\bullet}{m}_w} = C_w\int_{t_{w1}}^{t_{w2}}\frac{dt_w}{h_{sw}-h_a}\ldots\ldots\ldots\ldots(19)$$

$$\frac{ka.V}{\overset{\bullet}{m}_a} = \int_{h_{w1}}^{h_{w2}}\frac{dh_w}{h_{sw}-h_a}\ldots\ldots\ldots\ldots\ldots(20)$$

The above two equations are convertible in to one another and independent of real active motion of the two fluids streams. Mathematical integration of the equations is required and the procedure must account for relative motion. In cooling tower practice, the integrated value of equation (19) is called "The number of transfer units" or "NTU". This gives the number of times the average enthalpy potential ($h_{sw} - h_a$) goes in to the temperature chang of the water dh_w, thus one transfer unit has the definition of:

$$\frac{C_w.dt_w}{\left(h_{sw}-h_a\right)_{avg}} = 1\ldots\ldots\ldots\ldots\ldots\ldots(21)$$

In examining equation (19), it can be seen that the vertical distance between the two curves represents the enthalpy difference $\left(h_{sw}-h_a\right)$ in the integral of equation (19)[14]. Thus a second curve can be plotted for $1/(h_{sw}-h_a)$ as a function of the local water temperature, and the value of the integral can be determined by obtaining the area under the curve. The resulting quantity $(ka.V/m_w^{\bullet})$ known as the tower characteristic, is thus a function of the inlet and exit air wet bulb temperatures and the inlet and exit water temperatures. These can be expressed in terms of the approach temperature, the temperature range of the water, and the ratio of the water flow to the air flow rate. However the log-mean-enthalpy method based on the inlet and outlet enthalpy differences would underestimate the value of the tower characteristic, $ka.V/m_w^{\bullet}$, the enthalpy correction, dh, may be defined by equation (22).

$$dh=\frac{h_{sw1}+h_{sw2}-2h_{swm}}{4} \qquad \text{.........(22)}$$

where dh in Btu/LB, h_{sw1} and h_{sw2} are the values of h_{sw} at the outlet and inlet, and h_{swm} is the value of h_{sw} evaluated at the mean water temperature, $(t_{w1}+t_{w2})/2$, this is obtained from equation (23)[15].

$$h_{sw}=4.7926+2.568*t_w-0.029834*t_w^2+0.0016657*t_w^3 \qquad \text{..(23)}$$

If Δh_1 and Δh_2 are the inlet and outlet enthalpy differences between the h_{sw} and h_a curves, an approximate log-mean-enthalpy difference, Δh_m can now be defined as:

$$\Delta h_m=\frac{\Delta h_2-\Delta h_1}{2.3\log\{(\Delta h_2-dh)/(\Delta h_1-dh)\}} \qquad \text{.......................................(24)}$$

where Δh_1, and Δh_m in Btu/Ib.

The tower characteristic can be then calculated from equation below after multiply Δh_m by 0.4299.

$$\frac{ka.V}{m_w^{\bullet}}=\frac{t_{w2}-t_{w1}}{\Delta h_m} \qquad \text{.............(25)}$$

The error involved in estimating the tower characteristic using the corrected log-mean-enthalpy method is small and normally acceptable which is about 2 percent. The difference between the use and no use of the corrected log-mean-enthalpy method is about 23 percent. The results are plotted graphically and the best straight line through each set of points is drawn. The values of "n" and "l" would be approximated to 0.44 and 0.179 respectively and the characteristic equation becomes:

$$\frac{ka.V}{m_w^{\bullet}}=0.44\left(\frac{m_w^{\bullet}}{m_a^{\bullet}}\right)^{-0.179} \qquad \text{.......(26)}$$

5. RESULTS AND DISCUSSION

Fig. (2) shows the variation in water temperature with different heating load along the tower stages. At each tower stage the water in temperature will decrease with increase the air volume flow rate, and this is represented in Fig. (3). At each stage of the tower the temperature of water will increase with increase in the water mass flow rate. This is represented in Fig. (4). The air velocity vector field that is shown in Fig. (5) highlights the air flow along the tower. Fig. (6) shows the moist air density variation as it passes through the Hilton tower. The magnitude of this density depends on the magnitude of the static pressure and air dry bulb temperature. The air enthalpy variation as it passes through the Hilton tower is presented in Fig. (7). The variation in the air moisture content through Hilton tower is exhibited in Fig. (8). The variation in the water enthalpy through Hilton water cooling tower is shown in Fig. (9). The variation in the rates of heat transfer from warm water to bulk air as they flow through the Hilton tower is exhibited in Fig.(10). The variation in mass transfer rate from water to the bulk air as they flow through the Hilton tower is shown in Fig. (11).

The characteristic equations for these two types of packing are presented in equations (27) and (28) respectively[4].

$$\frac{kav}{\dot{m}_w} = 0.199\left(\dot{m}_w/\dot{m}_a\right)^{-0.592} ....(27)$$

$$\frac{kav}{\dot{m}_w} = 0.157\left(\dot{m}_w/\dot{m}_a\right)^{-0.388} ......(28)$$

The above two equations are used in the present theoretical work to predict the air and water properties that flow through these types of packing. This is done under the same inlet conditions (air and water temperatures and velocities) that are used in the experimental work. The theoretical packing-air resistance is similar to the Hilton tower packing-air resistance. Figs. (12 to 14) show the variation in the air enthalpy, moisture content and water enthalpy respectively, along (0.66 m) height ceramic packing [4]. Figs.(15 to 17) show the same above variables variation along (0.48 m) height ceramic packing [4]. Fig.(18) shows the variation of the water temperatures along the tower stages for the three types of packing. (I.e aluminum, ceramic of 1.27 m height and ceramic of 0.48 m height) it is clear from this figure that the water cooling range for the Hilton packing is greater than that of both ceramic types. This is because the coefficient of performance (ka) for the Hilton packing is greater than the other packing two types. It is found also that the increase in the packing height lead to increase the cooling range, since it allow for much time for direct contact between the warm water and bulk air.

The packing resistance to air flow was calculated and added to the y-direction momentum equation only. This is because of the assumption that there is no heat and mass transfer in the horizontal direction. Fig. (19) shows the variation of water temperatures with the use of the packing-air resistance. Fig. (20) shows the variation of the same variable without the use of the packing-air resistance. These two figures represent a simple comparison between the two states. This comparison highlight the effect of this resistance, so that the water cooling range in the first case (use of packing-air resistance) is more than the second case.

Many experimental tests are done by using a Hilton water cooling tower. Experimental results are compared with the theoretical results. The variation in the air enthalpy and water temperatures along the tower stages was considered in this comparison. Figs.(21 to 22). show the theoretical and the experimental water temperatures variation along the tower stages at different coefficient of performance (ka) values. The theoretical water cooling range is more than the experimental one in all these figures. This is due to the shape of the packing. That the simulation of this shape in the theoretical work is very complex, therefor the packing-air resistance which used in the numerical solution is not similar to the experimental packing-air resistance that actually exist inside the tower during the tests. However, the use of the theoretical resistance will decrease the difference between theoretical and experimental results. This comparison show a 7.69 % difference between these results. All these figures show that the delivery of experimental water temperature is higher than it in the final stage (one) is Fig. (23) shows the variation of delivery water temperature with the coefficient of performance (ka) values.

References

1. Majumdar, A. K.; Singhal, A. K. and Spalding, D. B. (1995). "Numerical modeling of wet cooling towers – Part1: Mathematical and Physical models". Journal of Heat Transfer. 105 P: 728 – 735.
2. Burger, R. (1989). "Improving cross – flow cooling tower operation". Hydrocarbon Processing. 68(12) P: 51 – 52.
3. Alwan, A. F (1991). "Experimental and numerical analysis of a counter – flow water cooling tower". M. Sc. Thesis College of Engineering. University of Baghdad.
4. Al – Habobi, M. A. (1995). "Performance of Different Packing Configurations In A Counter Flow Water Cooling Tower". M. Sc. Thesis. College of Engineering. University of Baghdad.
5. Mohiuddin, AKM. And Kant, K. (1996). "Knowledge base for the systematic design of wet cooling towers. 1. Selection and tower characteristics". International Journal of Refrigeration – Revne International du forid. 19(1) P: 43 – 51.
6. Al – Nimr, MA. (1998). "Dynamic thermal behavior of cooling towers". Energy conversion 2 management. 39(7) P: 631 – 636.
7. Bedekar, SV.; Nithiarasu, P. and Seetharamu, KN. (1998). "Experimental investigation of the performance of a counter – flow, Packing – bed mechanical cooling tower". Energy. 23(11) P: 943 – 947.
8. Gan, G. and Riffat, SB. (1999). "Numerical simulation of closed wet cooling towers for chilled ceiling systems". Applied Thermal Engineering. 19(12) P: 1279 – 1296.
9. Al – Nimr, MA. (1999). "Modeling the dynamic thermal behavior of cooling towers containing packing materials". Heat Transfer Engineering. 20(1) P: 91 – 96.
10. Abdullah, A. N. (2002). "Thermal analysis and numerical modeling for open – type forced – draft – water cooling towers". M. Sc. Thesis College of Engineering. University of Technology.
11. Versteeg, H. K. and Malalasekevq, W. (1995). "An introduction to

computational fluid dynamics the finite volume method". Longman Scientific and Technical. London.

12. Patankar, S. V. (1980). "Numerical heat transfer and fluid flow". Hemisphere publishing Corporation. New York.

13. Southworth, R. W. and Deleeuw, S. L. (1965). "Digital computation and numerical methods". Mcgraw – Hill book company. New York.

14. Fraas, A. P. and Necatiozisik M. (1965). "Heat Exchanger Design" John Wiley 2 sons, Inc. , New York.

15. Stoecker, W. F. and Jones, J. W. (1982). "Refrigeration and air conditioning". Mcgraw – Hill book company. London.

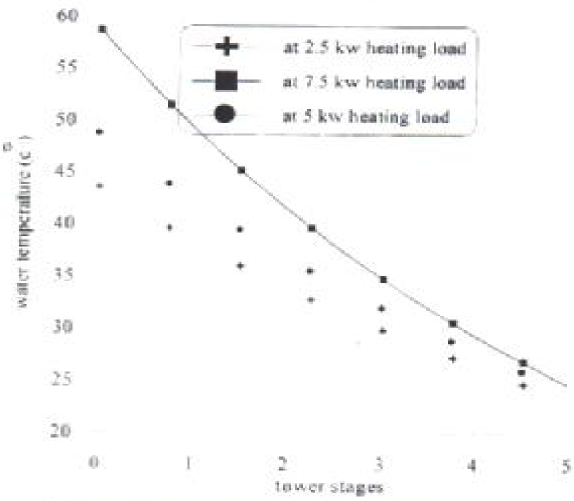

Figure (2):Variation of water temperature with different heatin- loads along cooling tower stages.

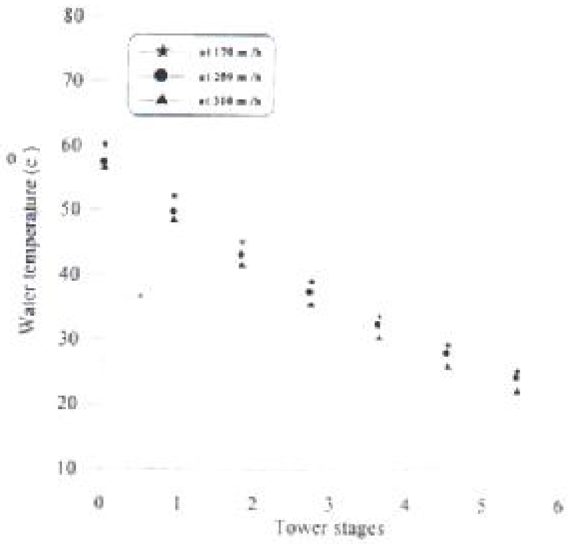

Figure (3): Variation of water temperature with different volume flow rates of incoming air along the cooling tower stages.

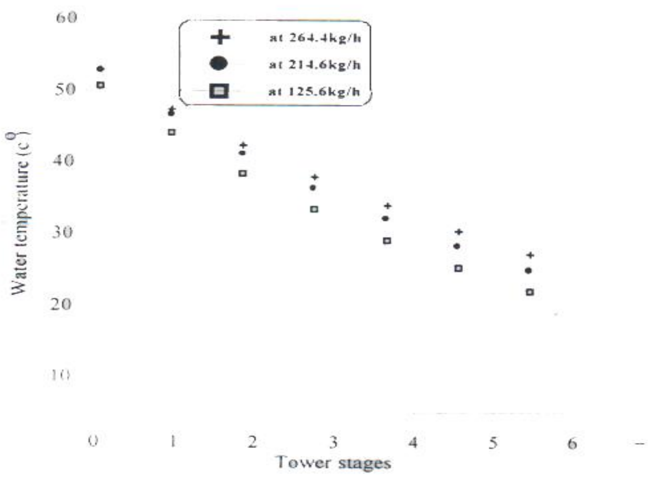

Figure (4): Variation of water temperature with different mass flow rates of interring water along the tower stages.

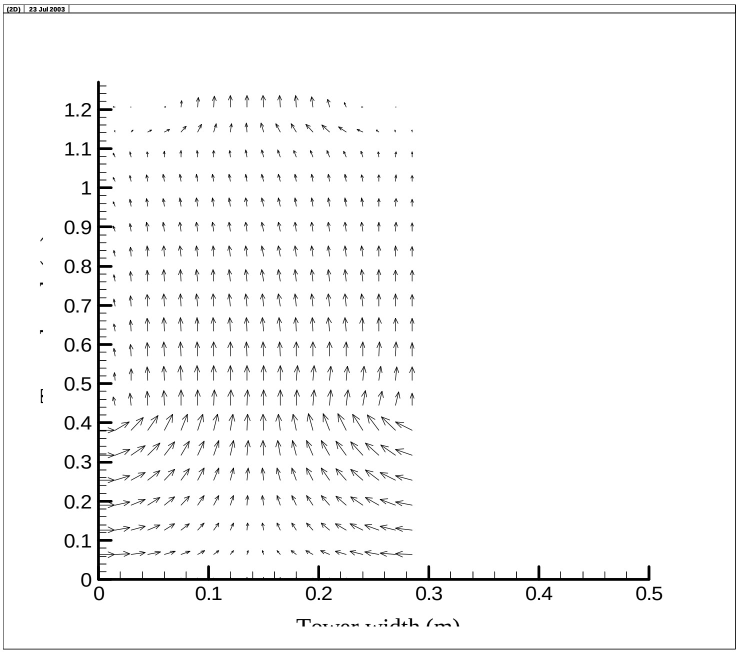

Figure (5): Air velocity vector field through the counter flow type water cooling tower.

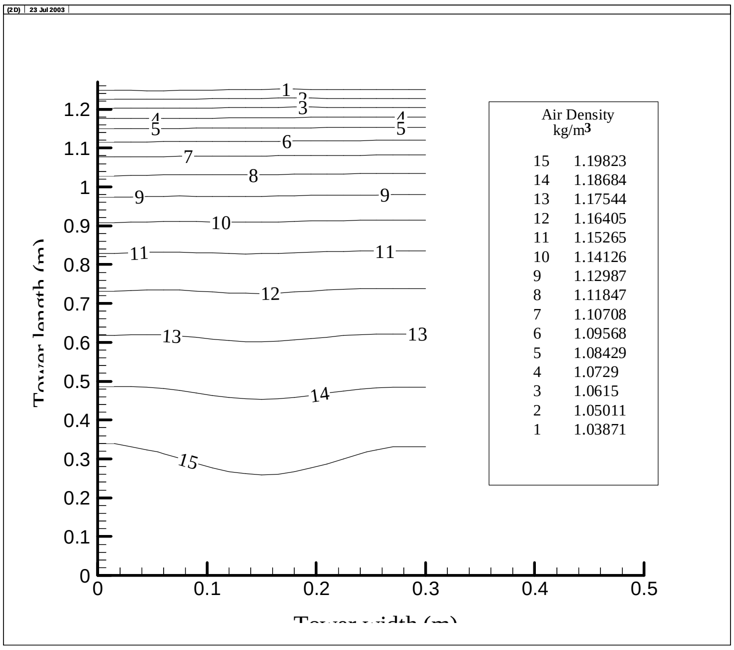

Figure (6): Moist air density contour through the counter flow type water cooling tower.

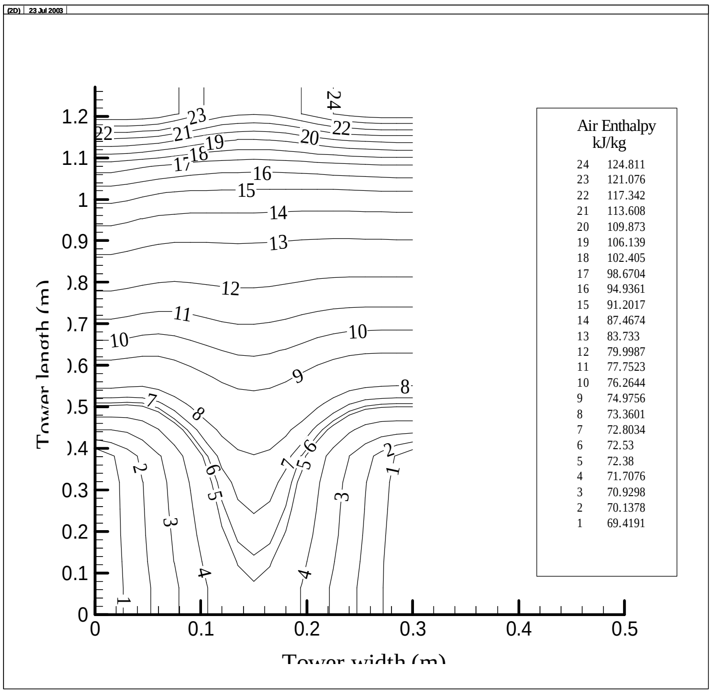

Figure (7): Air enthalpy contour through the counter flow type water cooling tower

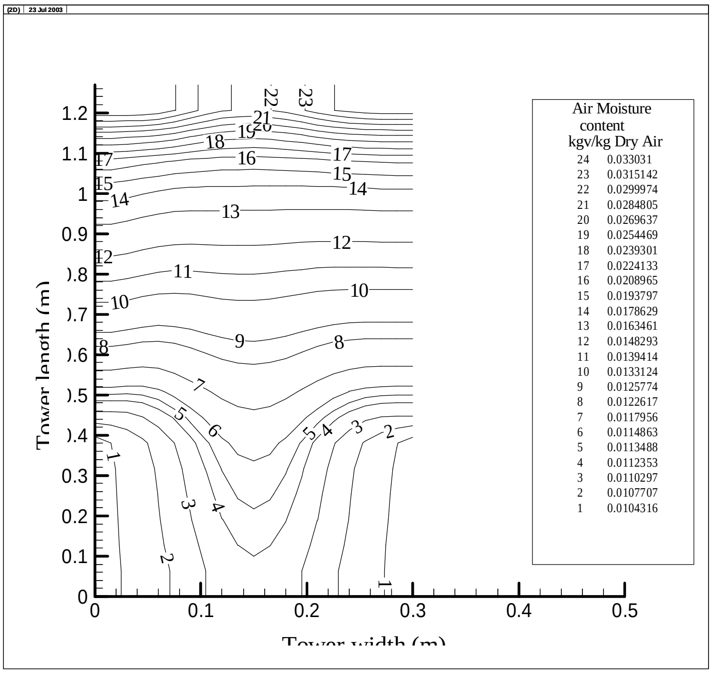

Figure (8): Air moisture content contour through the counter type water cooling tower.

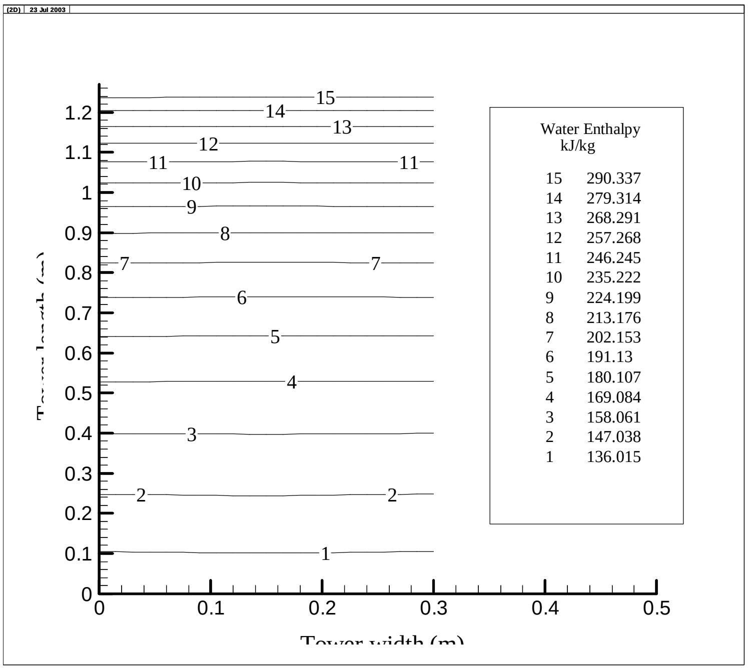

Figure (9): Water enthalpy contour through the counter type water cooling tower.

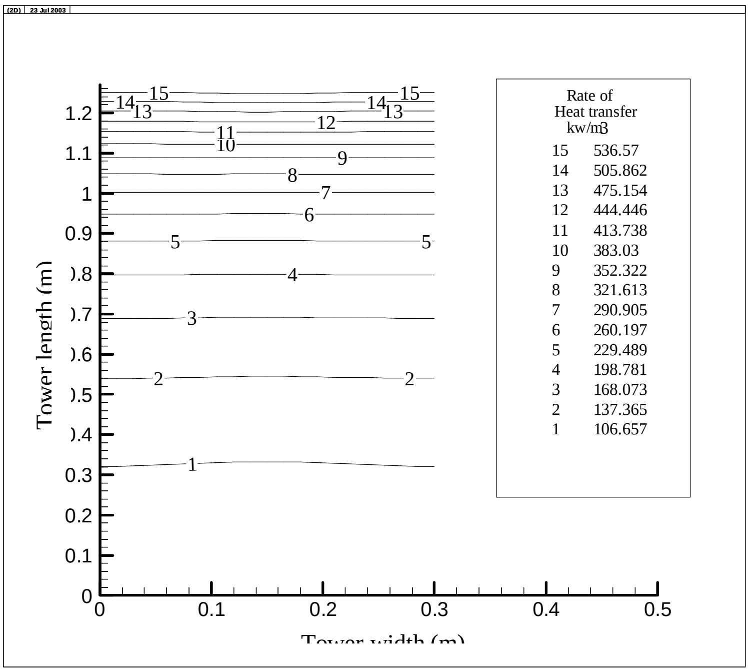

Figure (10): The rate of heat transfer contour through the counter type water cooling tower.

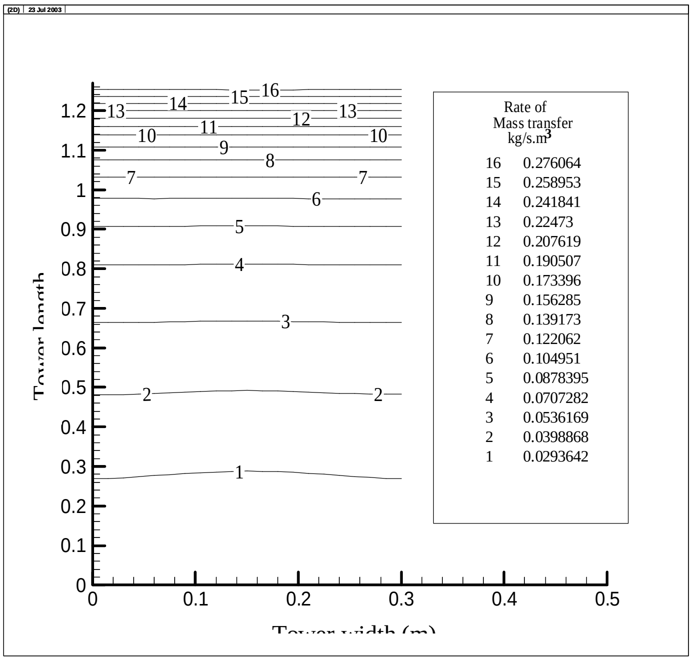

Figure (11): The rate of mass transfer contour through the counter flow type water cooling tower.

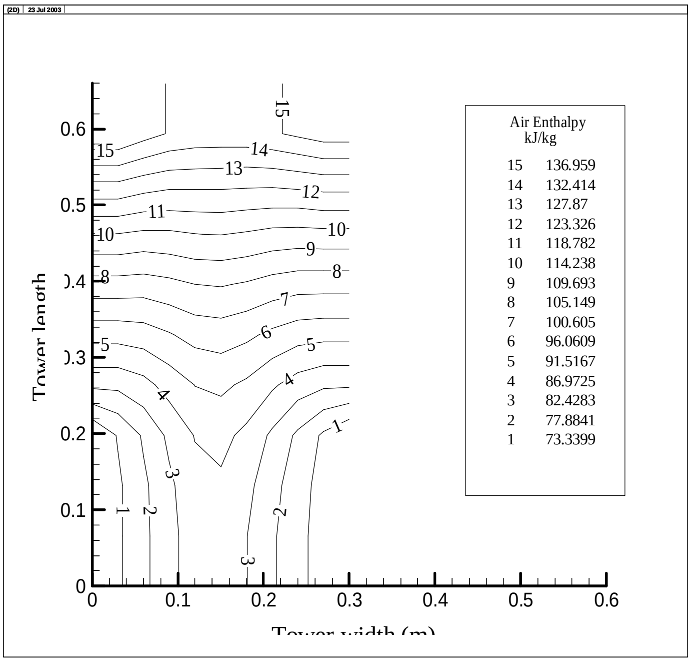

Figure (12): Air enthalpy contour through the counter flow type water cooling tower 0.66 m ceramic packing height.

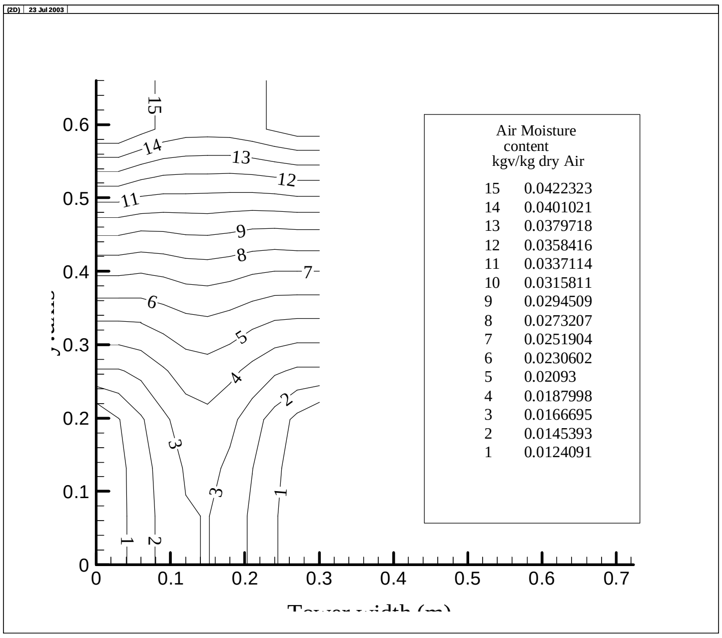

Figure (13): Air moisture content contour through the counter flow type water cooling tower at 0.66 m height ceramic packing type.

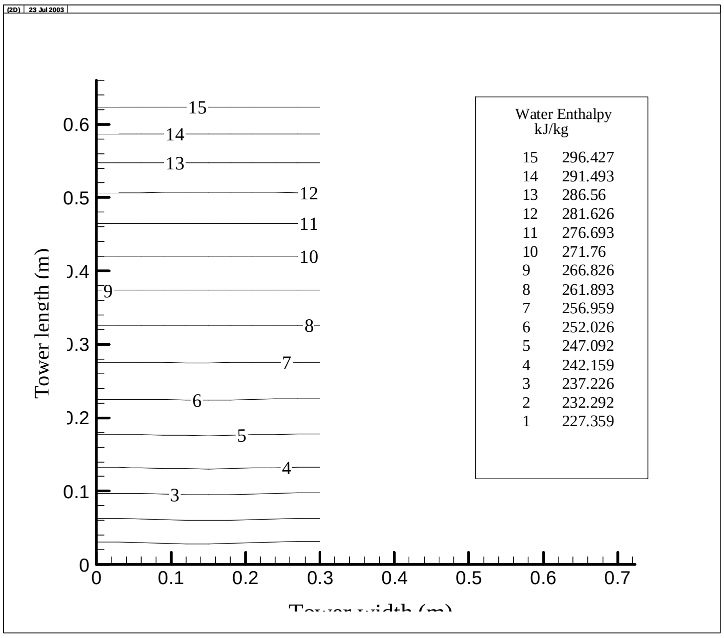

Figure (14): Water enthalpy contour through the counter flow type water cooling tower at 0.66 m ceramic packing height.

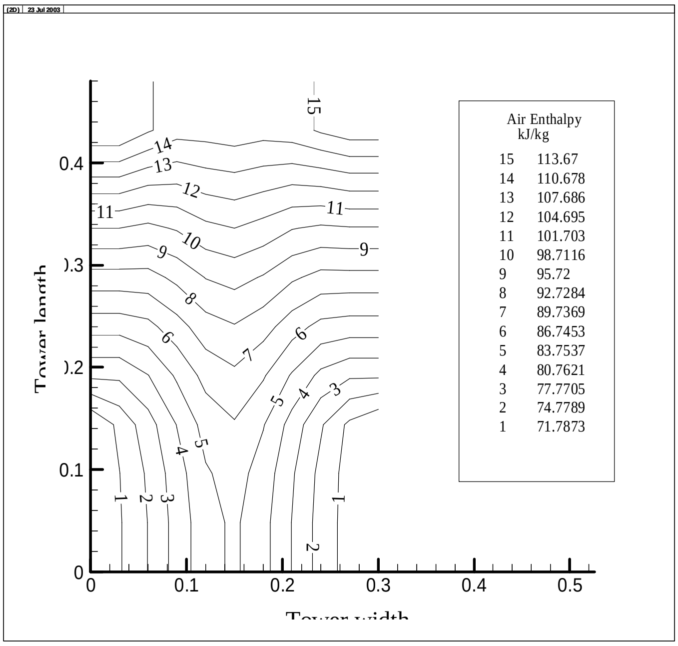

Figure (15): Air enthalpy contour through the counter flow type water cooling tower at 0.48 m ceramic packing height.

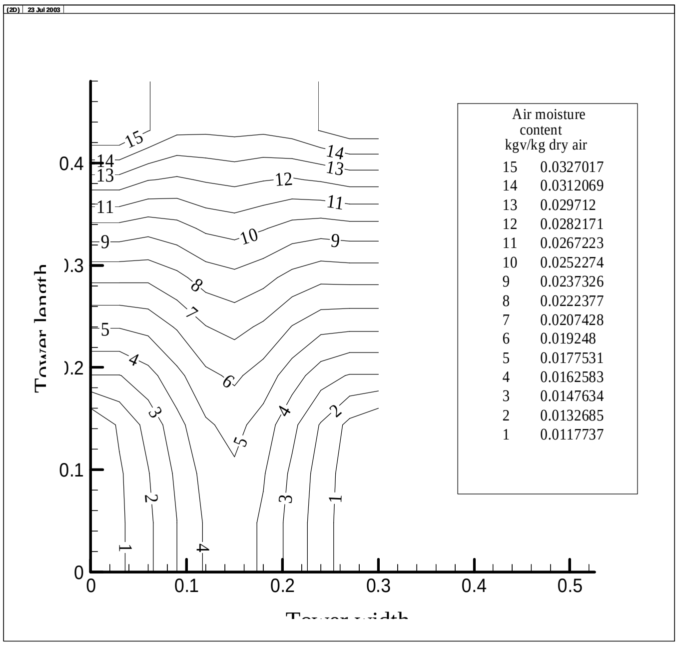

Figure (16): Air moisture content contour through the counter flow type water cooling tower at 0.48 m ceramic packing height.

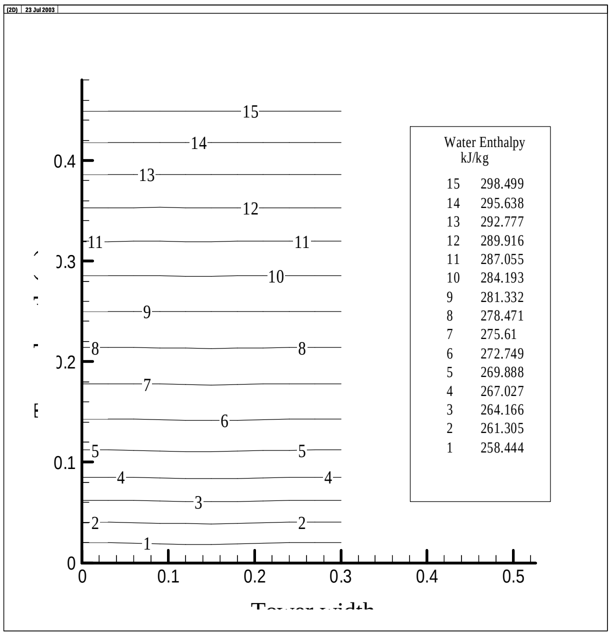

Figure (17): Water enthalpy contour through the counter flow type water cooling tower at 0.48 m ceramic packing height.

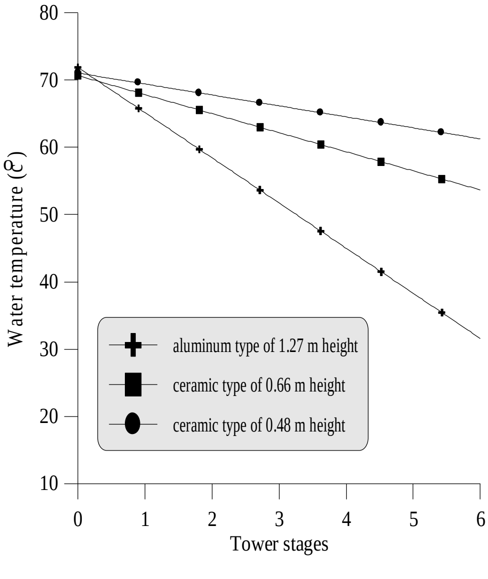

Figure (18): Variation of water temperature along the cooling tower stages at the use of aluminum packing time and ceramic packing in two different heights at another time.

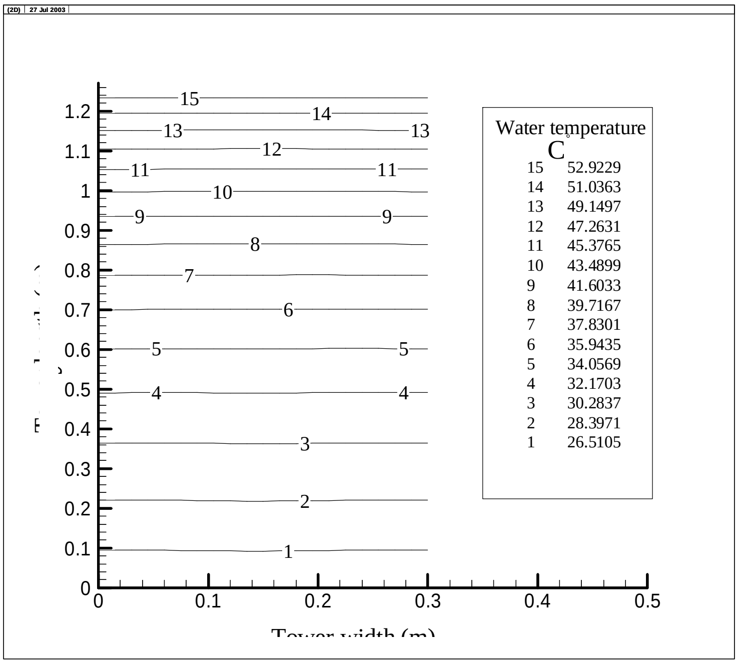

Figure (19): Water temperature contour with using the packing air resistance.

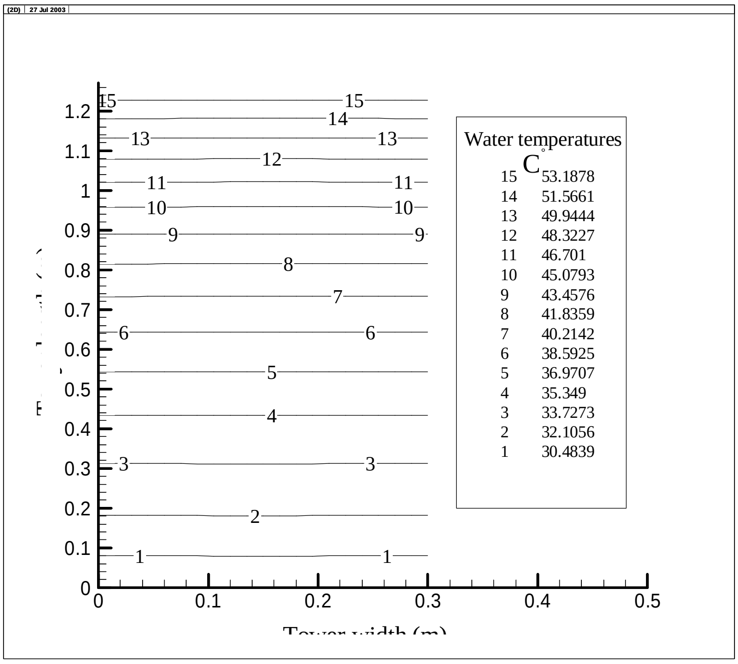

Figure (20): Water temperature contour without using the packing air resistance.

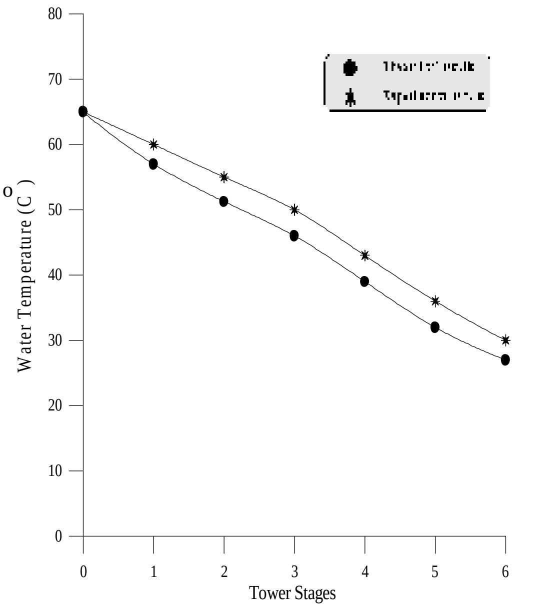

Figure (21): The theoretical and experimental variation of water temperatures along the tower stages at $ka = 0.1414\ (\frac{kg}{m^3.\sec})$.

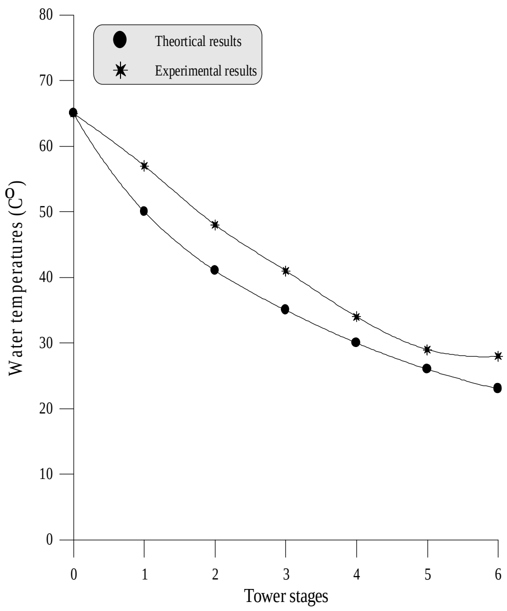

Figure (22): The theoretical and experimental variation of water temperatures along the tower stages at $ka = 0.1567(\frac{kg}{m^3.\sec})$.

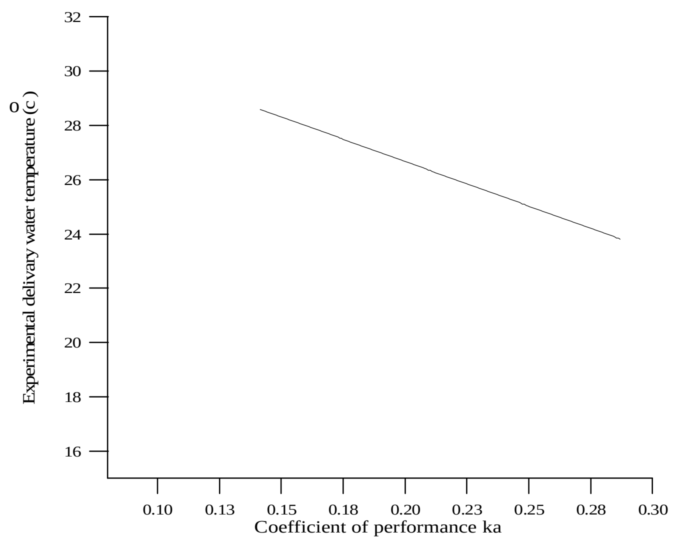

Figure (23): Variation of delivery water temperature with coefficient of performance (ka).